

# Orthogonal Test Design for Optimisation of the Carbon-based Nickel Electrodeposits as Cathode Catalysts for Hydrogen Evolution in Microbial Electrolysis Cell

Yu Zhao\*, Zhishuai Dong, Yuxue Wang, Donghua Yang, Xia An

College of Chemistry and Chemical Engineering, Taiyuan University of Technology, Taiyuan, Shanxi, P. R. China, 030024

\*E-mail: [tyut1995@126.com](mailto:tyut1995@126.com), [zhaoyu@tyut.edu.cn](mailto:zhaoyu@tyut.edu.cn)

Received: 23 November 2018 / Accepted: 7 January 2019 / Published: 7 February 2019

Nickel particles coating was electrodeposited on carbon paper (CP) surface to form carbon-based nickel, which was then used as the cathodic catalyst in MEC to evolve hydrogen production. The primary electrodeposition parameters of electrolyte concentration of nickel sulphate, imposed current density, and plating time were considered. An orthogonal test was designed based on three factors and three levels. Results showed that the optimal operating parameters were as follows: 30 g L<sup>-1</sup> nickel sulfate, 12 A m<sup>-2</sup> imposed current density, and 10 min of plating time. The chemical composition and morphology characteristics were revealed using XRD and SEM, respectively. In addition, the carbon-based nickel was obtained under the optimal electrodeposition parameters and used as cathode in a stably running microbial electrolysis cell. The evolved gas volume was 8.1 ± 0.1 mL, the hydrogen content was 82.6 ± 2.1%.

**Keywords:** Orthogonal experiment; electrodeposition; Carbon-based nickel; Hydrogen Evolution

## 1. INTRODUCTION

Hydrogen is recognised as the most important renewable energy of the future because of its high energy content per unit and clean combustion [1]. Scholars have focused on the hydrogen production and proposed numerous methods, such as fossil fuel reforming [2], water electrolysis [3], fermentation [4], and photocatalytic water splitting [5], however, these methods are unsustainable for a long-term [6-8]. Biohydrogen by microbial electrolysis cell (MEC) is a promising approach for hydrogen production along with the utilisation of wastes or other renewable substrates as organic matter [9].

Hydrogen is produced at the cathode through the hydrogen evolution reaction (HER) in MEC [10]. The choice of cathode, i.e. catalyst and material, is the most important part of the MEC. Precious platinum has been recognised as the most effective catalyst because of its low HER over-potential loss in MEC, however the high cost and poisoning (by sulphides, alcohols, phosphate anions, or carbon monoxide) limit its extensive application [11-13]. Therefore, numerous cathode materials have focused on developing to replace Pt, including MoS<sub>2</sub> [14], stainless steel [15], Ti [16], Pd [17], and Cu [18]. However, nickel or nickel alloy have considerable advantages due to its low HER over-potential, high efficiency, and low cost [19-22]. NiMo and NiW cathode were prepared by electrodepositing on a carbon-fibre-weaved cloth, which showed excellent hydrogen production performance [19]. Selembó demonstrated that Ni 625 was better than other nickel alloys (i.e., Ni 201, Ni 400, and Ni HX) [20]. According to Jeremiasse [21], Ni foam had low cathodic overpotential compared with Pt-based cathode. Kadier observed that the electroformed Ni mesh catalysts as a viable cathode material had considerable potential for hydrogen production in MECs [22]. Electrodeposition is acknowledged as a technically feasible method, due to the following qualities: low cost equipment, normal pressure, room temperature, rapid deposition, and simple operation [23].

In this study, nickel particle coating was formed on carbon paper (CP) surface through constant current electrodeposition and used as cathodic catalyst in a MEC to advance hydrogen production. An orthogonal test was designed to determine the optimum electrodepositing parameters. The most important operating parameters, namely, the concentration of nickel sulphate, imposed current density, and plating time were selected as three factors, along with three levels under every factor. L<sub>9</sub> orthogonal array was considered for this work. Then the prepared samples were employed as cathode in MEC, of which hydrogen production performance was comprehensively expressed by generated current density, gas volume, and hydrogen content. The factors were ranked by order based on mathematical model. Then, the optimal combination of the three factors and three levels were selected through multifaceted analysis. Under the optimal plating conditions, carbon-based nickel (Ni) was prepared to act as MEC cathode. Finally, its hydrogen evolution performance and electrochemical behaviour were explored.

## 2. MATERIALS AND METHODS

### 2.1 Pretreatment of substrates

Firstly, the carbon paper (CP) substrates ( $2 \times 2 \text{ cm}^2$ ) were submerged in an acid solution of 0.5 mol L<sup>-1</sup> HCl at 25 °C for 2 h to remove the oxide layer on the surfaces; Secondly, the substrates were immersed in an alkaline solution of 0.5 mol L<sup>-1</sup> NaOH at 25 °C for 2 h to eliminate grease; Then, the substrates were immersed in deionised water for 5 h until a constant pH was achieved; Finally, these substrates were dried at 25 °C overnight to obtain the pretreatment CP.

## 2.2. Constant current electrodepositing

A watts-type nickel solution was used as electrolyte [24]. It was composed of 15 g L<sup>-1</sup> nickel chloride ( $\text{NiCl}_2 \cdot 6\text{H}_2\text{O}$ ) and nickel sulphate ( $\text{NiSO}_4 \cdot 6\text{H}_2\text{O}$ ) acting as ions source, 33 g L<sup>-1</sup> boracic acid ( $\text{H}_3\text{BO}_3$ ) as pH buffer and 0.5 g L<sup>-1</sup> sodium dodecyl benzene sulfonate (SDBS) as anti-pitting additive. The pretreated CP was utilised as cathode, a platinum mesh ( $2 \times 2 \text{ cm}^2$ ) as the anode with magnetic stirring in a water bath kettle at 25 °C. The distance between the cathode and anode is 4 cm. The CP was electrodeposited under different current densities by a direct current power (HB 17301 SL, Hossoni, Inc., China), and then washed thoroughly by deionised water, dried in air and finally heat-treated at 60 °C for 2 h. Thus, carbon-based nickel materials were obtained.

## 2.3 Design for orthogonal test

The primary electroplating parameters of current density, plating time and nickel sulphate concentration ( $\text{NiSO}_4 \cdot 6\text{H}_2\text{O}$ ) were considered in this study. L<sub>9</sub> orthogonal array was chosen for experimental design based on three plating parameters and three levels [25]. The factors and levels of the orthogonal experiment are listed in Table 1, and the L<sub>9</sub> orthogonal arrays are presented in Table 2.

**Table 1.** Factors and levels of the orthogonal experiment

Levels	A concentration of nickel sulphate (g L <sup>-1</sup> )	B imposed current density (A m <sup>-2</sup> )	C plating time (min)
1	30	4	5
2	50	8	10
3	70	12	15

**Table 2.** Schemes of the orthogonal experiment

Number	A concentration of nickel sulphate (g L <sup>-1</sup> )	B imposed current density (A m <sup>-2</sup> )	C plating time (min)
	Factors		
1	1	1	1
2	1	2	2
3	1	3	3
4	2	1	1
5	2	2	2
6	2	3	3
7	3	1	1
8	3	2	2
9	3	3	3

## 2.4 Hydrogen producing test

A single-chamber MEC, which used glucose  $1\text{ g L}^{-1}$  as electron donor, had run stably for one year. The working volume was 100 mL. The inoculated sludge came from a local coking wastewater treatment plant. Mature biofilm on carbon felt ( $2\text{ cm} \times 5\text{ cm} \times 1\text{ cm}$ ) was used as bio-anode, and Pt mesh as cathode. The electrolyte comprised the following (in 1000 mL distilled water): 5.618 g NaH<sub>2</sub>PO<sub>4</sub>, 6.155 g Na<sub>2</sub>HPO<sub>4</sub>, 0.13 g KCl, 0.31 g NH<sub>4</sub>Cl, and 12.5 mL trace metal solution [26]. The power source (HB 17301 SL; Hossoni, Inc., China) was supplied to the anode and cathode with voltage of 0.7 V. The MEC took batch mode. The prepared carbon-based nickel ( $2\text{ cm} \times 2\text{ cm}$ ) was utilised to replace Pt mesh as cathode, to explore its performance of electrochemically catalysed hydrogen evolution.

## 2.5 Electrochemical measurement

All electrochemical measurements were conducted through a V3 electrochemical workstation (Princeton, USA). A prepared carbon-based nickel was used as working electrode, a Pt net was applied as counter electrode, and a AgCl/Ag was employed as reference electrode. Linear sweep voltammetry (LSV) measurements and Tafel analysis were performed with a potential range of - 0.9 to 0.5 V and - 0.9 V to 0.1V at a scan rates of  $10\text{ mV s}^{-1}$  and  $5\text{ mV s}^{-1}$ , respectively.

## 2.6 Analysis of gas

Gas production in the MEC was measured by water replacement utilising a graduated flask. The gas composition was analysed by a gas chromatograph (Thermo Fisher Scientific, Waltham, MA, USA).

## 2.7 XRD and SEM analysis

The morphologies and chemical composition of the composites were investigated by SEM (JSM-7001F, JEOL, Japan) and XRD (XRD-6000, Shimadzu LabX, Japan), respectively.

# 3. RESULTS AND DISCUSSION

## 3.1 Orthogonal test

As shown in Table 3, the value of K is the sum of experimental results with the corresponding level under each factor. R is the value of the maximum minus the minimum of K for each factor. The influences of three factors on the generated current density, volume of produced gas and hydrogen content can be ranked as follows: C > A > B, A > C > B, and A > B > C, respectively [27].

**Table 3.** Results of the orthogonal test

Orthogonal test for electrodeposition				MEC performance		
samples	nickel sulphate (g L <sup>-1</sup> )	imposed current density (A m <sup>-2</sup> )	plating time (min)	gas volume (mL)	hydrogen content (%)	generated peak current density (A m <sup>-2</sup> )
1	30	4	5	6.2	82	10.00
2	30	8	10	7.9	78	12.56
3	30	12	15	2.0	88	5.33
4	50	4	5	4.4	79	7.85
5	50	8	10	1.7	67	6.45
6	50	12	15	4.1	76	8.05
7	70	4	5	2.2	78	6.13
8	70	8	10	2.3	76	5.93
9	70	12	15	0.2	76	8.90
gas volume /mL	K1	16.10	12.80	12.60		
	K2	10.20	11.90	12.50		
	K3	4.70	6.30	5.90		
	$\bar{K}1$	5.37	4.27	4.20		
	$\bar{K}2$	3.40	3.97	4.17		
	$\bar{K}3$	1.57	2.10	1.97		
	R	3.80	2.17	2.23		
gas composition	K1	2.48	2.39	2.34		
	K2	2.22	2.21	2.33		
	K3	2.30	2.40	2.33		
	$\bar{K}1$	0.83	0.80	0.78		
	$\bar{K}2$	0.74	0.74	0.78		
	$\bar{K}3$	0.77	0.80	0.78		
	R	0.09	0.06	0.00		
the maximum current density/ A m <sup>-2</sup>	K1	27.89	23.98	23.98		
	K2	22.35	24.94	29.31		
	K3	20.95	22.28	17.90		
	$\bar{K}1$	9.30	7.99	7.99		
	$\bar{K}2$	7.45	8.31	9.77		
	$\bar{K}3$	6.98	7.43	5.97		
	R	2.31	0.89	3.80		

Therefore, the generated current density was most influenced by plating time, followed by the concentration of nickel sulphate and imposed current density, of which the largest concentration ( $12.55 \text{ A m}^{-2}$ ) was achieved from the orthogonal experiment as follows: A2 B2 C2. Meanwhile, the volume of produced gas was primarily affected by the imposed current density, followed by the plating time and concentration of nickel sulphate, the largest gas volume (7.9 mL) was achieved from A1 B2 C2. Lastly, the hydrogen content of produced gas was mainly controlled by nickel sulphate concentration, followed by the imposed current density and plating time, the largest hydrogen content (88%) was achieved from the orthogonal experiment as follows: A1 B3 C3.

If the generated current density was assigned as the evaluation criteria, then the maximum of K1 ( $27.89 \text{ A m}^{-2}$ ) was obtained corresponding to the optimal level A1 from factor A column; the maximum of K2 ( $24.94 \text{ A m}^{-2}$ ) was received for factor B column, which was closely related with the optimal level B2. From factor C column, the maximum of K2 ( $29.31 \text{ A m}^{-2}$ ) was relevant to the optimal level C2. Considering the generated current density, A1 B2 C2 was recognised as the optimal electrodeposition parameters. Similarly, A1 B1 C1 was the optimal operating parameters using gas volume as indicator, whilst A1 B3 C1 was the best involved in hydrogen content.

In summary, three factors were comprehensively evaluated to obtain the optimal electrodeposition operating parameters: (1) A1 was the best choice owing to its simultaneous selection in three optimisation combinations. (2) The large variation of intensity (rise and fall) meant the large impact of factor (Fig.1), factor B had the largest impact on hydrogen content, generated current density and gas volume making B3 the best choice involving the hydrogen composition. (3) The order of impact for factor C was the generated current density, gas volume and hydrogen content, which denoted that C1 was the best choice. However, producing hydrogen is the ultimate goal in MEC, therefore, C2 was carefully selected as the best factor and not C1.

Finally, the optimum electrodepositing parameter was A1 B3 C2, that is, the concentration of nickel sulphate,  $30 \text{ g L}^{-1}$ ; the imposed current density,  $12 \text{ A m}^{-2}$ ; and the plating time, 10 min.

### *3.2 Electrochemical performance and characterisation*

Under the former optimum electrodepositing condition, the carbon-based nickel was prepared and then used as cathode in the stably running MEC to study its electrochemical performance.

#### *3.2.1 Performance of producing electricity*

The variation of generated current density of seven batches with time was shown in Fig. 1A. At every batch, the maximum of generated current density was rapidly reached within approximately 0.5 h and then lasted for 20 h, finally demonstrating a gradual decrease. With the running of MEC, the peak current density slightly from  $14.74 \text{ A m}^{-2}$  of the 1st cycle to  $14.83 \text{ A m}^{-2}$  of the 7th cycle, which meant that the MEC ran very smoothly.

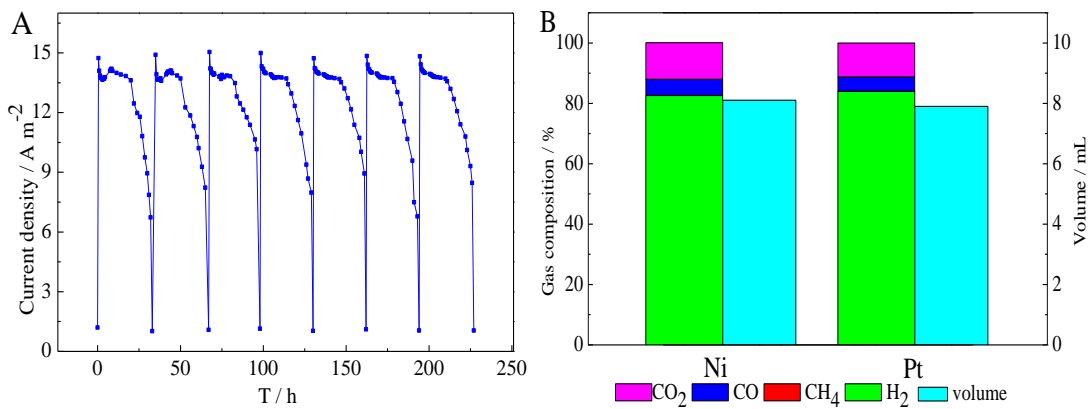


**Figure 1.** (A) Generated current density-time curves of seven batches. (B) The average volume and composition of produced gas in the 5th to 7th batches.

From Fig. 1B, the volume of produced gas from carbon-based nickel in a batch was  $8.1 \pm 0.1$  mL, which was 2.5% higher than that of platinum mesh cathode ( $7.9 \pm 0.1$  mL) with equal area. The composition of produced gas from MEC comprised  $\text{H}_2$ ,  $\text{CH}_4$ ,  $\text{CO}$  and  $\text{CO}_2$ . The hydrogen content from nickel ( $82.6 \pm 2.1\%$ ) was slightly lower than that of platinum mesh ( $83.9 \pm 1.5\%$ ). That is, carbon-based nickel produced slightly more hydrogen (6.7 mL) than platinum mesh (6.6 mL). Kadier [28] obtained the cathode of Ni mesh by electroforming, under the external voltage of 1.1V, the hydrogen production rate of  $4.18 \text{ H}_2 \text{ m}^3 \cdot \text{m}^{-3} \cdot \text{d}^{-1}$  was obtained and the coulomb efficiency was 75 %. Hrapovic [29] made Ni particles as cathode catalysts by electrodeposition method and obtained the hydrogen production rate of  $5.4 \text{ m}^3 \text{ H}_2 \cdot \text{m}^{-3} \cdot \text{d}^{-1}$  under the applied voltage of 1 V. Jeremiasse [30] found that using foam Ni as the cathode, the hydrogen production rate was  $5 \text{ m}^3 \text{ H}_2 \cdot \text{m}^{-3} \cdot \text{d}^{-1}$  at an external voltage of 1 V.

### 3.2.2 Electrochemical performance

The electrochemical property of Ni and Pt cathodes was characterised by LSV [31] (Fig. 2A). As shown in Fig. 2A, the Ni cathode exhibited a current density of  $-41.3 \text{ A m}^{-2}$  at a potential of  $-0.899$  V (vs.  $\text{AgCl} / \text{Ag}$ ), which was higher than that of Pt cathode ( $-38.8 \text{ A m}^{-2}$ ). This finding demonstrated that the former had higher electrochemical activity.

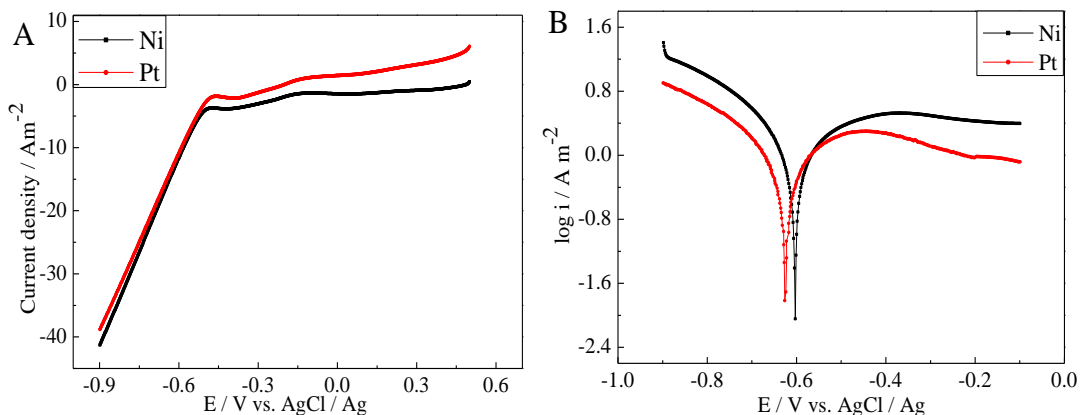


**Figure 2.** (A) Linear sweep voltammetry (LSV) curves with a potential range of 0.6 V to - 0.9 V at a scan rate of 5  $\text{mV s}^{-1}$ . (B) Polarization curves with supposing  $\Delta E$  of 5.0 mV over electric potential scanning range from - 0.9 V to - 0.1 V.

Tafel analysis was used to study the electrode kinetics by determining the exchange current density ( $i^0$ ) and the equilibrium potential ( $E^0$ ) [32].  $E^0$  refers to the potential, at which forward and reverse reaction speed on electrode are equal;  $i^0$  represents the maximum reaction rate at equilibrium potential, a high value of  $i^0$  denotes a fast reaction rate, following a low activation energy barrier of forward reaction. HER is easy with the increase in  $i^0$ . From Fig. 2B, the equilibrium potential of Ni and Pt electrodes was - 0.604 V and slightly - 0.626 V, respectively. The  $i^0$  of Ni and Pt cathodes was 2.52 and 2.37  $\text{A m}^{-2}$ , respectively.

### 3.2.3 XRD and SEM

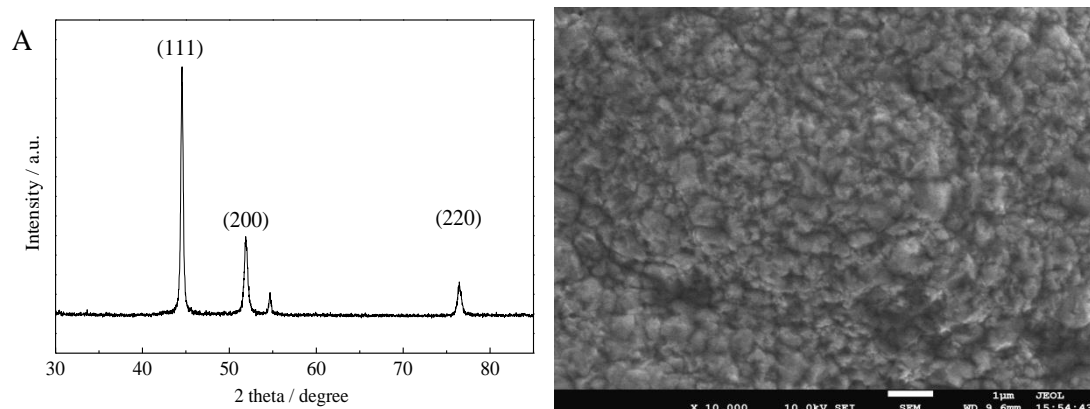


**Figure 3.** (A) XRD pattern and (B) SEM of carbon-based nickel.

As shown in Fig. 3A, three diffraction peaks can be found at  $2\theta$  values of  $44.52^\circ$  (111),  $51.88^\circ$  (200), and  $76.46^\circ$  (220), respectively, which are corresponding to Ni (JCPDSNO.65-2865). The value of unit cell parameters was 0.124 nm, and the value of crystalline interplanar spacing was 0.203 nm. From Fig. 3B, it was observed that the coating deposited on CP surface was rough, and accumulated like ‘prismatic-like stones’ with hierarchical structure.

#### 4. CONCLUSIONS

The optimal electrodepositing parameters (the concentration of nickel sulphate, 30 g L<sup>-1</sup>; the imposed current density, 12 A m<sup>-2</sup>; the plating time, 10 min) were obtained through a orthogonal test. The carbon-based nickel was prepared and used as cathode in a MEC. The chemical composition of the carbon-based nickel was demonstrated by XRD test. A total of 6.7mL of hydrogen was produced at an applied voltage of 0.7 V, and had superior hydrogen-producing capacity to Pt mesh. However, the price of platinum net is 400 times more than carbon-based nickel with the same area. Considering the low cost and abundance of Ni, especially with regard to the superior electrochemical performance, carbon-based Ni demonstrates considerable potentials for application in MECs.

#### ACKNOWLEDGEMENTS

This work was funded by the Provincial Natural Science Foundations of Shan xi, China (2014011014-6, 201701D121028). The authors also acknowledged the Institute of Coal Chemistry, Chinese Academy of Sciences for technical assistance.

#### References

1. R. Chaubey, S. Sahu, O. O. James and S. Maity, *Renew. Sust. Energy. Rev.*, 23 (2013) 443.
2. M. Steinberg and H. C. Cheng, *Int. J. Hydrogen Energy*, 14 (1989) 97.
3. A. Ursua, L. M. Gandia and P. Sanchis, *P. IEEE.*, 100 (2012) 410.
4. P. C. Hallenbeck, *Int. J. Hydrogen Energy*, 34 (2009) 7379.
5. X. Chen, S. Shen, L. Guo and S. S. Mao, *Chem. Rev.*, 110 (2010) 6503.
6. S. N. A. Rahman, M. S. Masdar, M. I. Rosli, E. H. Majlan, T. Husaini, S. K. Kamarudin and W. R. W. Daud, *Renew. Sust. Energy. Rev.*, 66 (2016) 137.
7. S. Manish and R. Banerjee, *Int. J. Hydrogen Energy*, 33 (2008) 279.
8. A. Kadier, M. S. Kalil, P. Abdeshahian, K. Chandrasekhar, A. Mohamed, N. F. Azman, W. Logroño, Y. Simayi and A. A. Hamid, *Renew. Sust. Energy. Rev.*, 61 (2016) 501.
9. X. Guo, J. Liu and B. Xiao, *Int. J. Hydrogen Energy*, 38 (2013) 1342.
10. R. K. Brown, U. C. Schmidt, F. Harnisch and U. Schröder, *J. Power Sources*, 356 (2017) 473.
11. H.Y. Dai, H. M. Yang, X. Liu, X. Jian and Z. H. Liang, *Fuel*, 174 (2016) 251.
12. P. A. Selembo, M. D. Merrill, B. E. Logan, *Int. J. Hydrogen Energy*, 35 (2010) 428.
13. M. Su, L. Wei, Z. Qiu, G. Wang and J. Shen, *J. Power Sources*, 301 (2016) 29.
14. H. Yuan, J. Li, C. Yuan and Z. He, *ChemElectroChem.*, 1 (2014) 1828.
15. D. F. Call, M. D. Merrill and B. E. Logan, *Environ. Sci. Technol.*, 43 (2009) 2179.
16. A.W. Jeremiasse, J. Bergsma, J. M. Kleijn, M. Saakes, C. J. Buisman, M.C. Stuart and H.V. Hamelers, *Int. J. Hydrogen Energy*, 36 (2011) 10482.
17. Y. X. Huang, X.W. Liu, X. F. Sun, G. P. Sheng, Y. Y. Zhang, G. M. Yan, S. G. Wang, A.W. Xu and H. Q. Yu, *Int. J. Hydrogen Energy*, 36 (2011) 2773.
18. T. Sangeetha, Z. Guo, W. Liu, M. Cui, C. Yang, L. Wang and A. Wang, *Int. J. Hydrogen Energy*, 41 (2016) 2189.
19. H. Hu, Y. Fan and H. Liu, *Int. J. Hydrogen Energy*, 34 (2009) 8535.
20. P. A. Selembo, M. D. Merrill, and B. E. Logan, *J. Power Sources*, 190 (2009) 271.
21. A.W. Jeremiasse, H.V. Hamelers, M. Saakes and C.J. Buisman, *Int. J. Hydrogen Energy*, 35 (2010) 12716.
22. A. Kadier, Y. Simayi, K. Chandrasekhar, M. Ismail and M. S. Kalil, *Int. J. Hydrogen Energy*, 40 (2015) 14095.

23. L. Shi, C. F. Sun, F. Zhou and W. M. Liu, *Materials Science and Engineering: A*, 397 (2005) 190.
24. H. Alimadadi, A. B. Fanta, T. Kasama, M. A. Somers and K. Pantleon, *Surf. Coat. Tech.*, 299 (2016) 1.
25. S. Li, Y. Li, J. Shi, T. Zhao and J. Yang, *Ecol. Eng.*, 102 (2017) 527.
26. H. Liu, R. Ramnarayanan and B. E. Logan, *Environ. Sci. technol.*, 38 (2004) 2281.
27. J. Gao, J. Yin, F. Zhu, X. Chen, M. Tong, W. Kang, Y. Zhou and J. Lu, *J. Taiwan Inst. Chem. E.*, 64 (2016) 196.
28. A. Kadier, Y. Simayi, K. Chandrasekhar, M. Ismail and M. S. Kalil, *Int. J. Hydrogen Energy*, 40 (2015) 14095.
29. S. Hrapovic, M. F. Manuel, J. H. T. Luong, S. R. Guiot and B. Tartakovsky, *Int. J. Hydrogen Energy*, 35 (2010) 7313.
30. A. W. Jeremiasse, H. V. M. Hamelers, M. Saakes and C. J. N. Buisman, *Int. J. Hydrogen Energy*, 35 (2010) 12716.
31. L. Wang, W. Liu, Z. He, Z. Guo, A. Zhou and A. Wang, *Int. J. Hydrogen Energy*, 42 (2017) 19604.
32. T. Xiang, S. Ding, C. Li, S. Zheng, W. Hu, J. Wang and P. Liu, *Mater. Design.*, 114 (2017) 65.

© 2019 The Authors. Published by ESG ([www.electrochemsci.org](http://www.electrochemsci.org)). This article is an open access article distributed under the terms and conditions of the Creative Commons Attribution license (<http://creativecommons.org/licenses/by/4.0/>).